# Interaction-induced supercurrent in quantum Hall setups

Xiao-Li Huang and Yuli V. Nazarov

*Kavli Institute of NanoScience, Delft University of Technology, Lorentzweg 1, NL 2628 CJ, Delft, The Netherlands*

Recently, we have proposed an unusual mechanism of superconducting current that is specific for quantum Hall edge channels connected to superconducting electrodes. We have shown that the supercurrent can be mediated by a nonlocal electron-electron interaction that provides an opportunity for a long-distance information transfer in the direction opposite to the electron flow. A convenient model for such interaction is that of an external circuit. The consideration has been performed for the case of a single channel. In order to facilitate the experimental verification and the observation of peculiar features of the effect, in this paper, we provide a more detailed description of the phenomenon and extend the results to more sophisticated setups. We establish that the dynamical phase contributes to superconducting interference; this being the manifestation of the channel chirality. We consider setups that include the scattering between quantum Hall channels of opposite direction and multiple superconducting contacts. For a single quantum Hall constriction, we derive a general and comprehensive relation for the interaction-induced supercurrent in terms of scattering amplitudes and demonstrate the nonlocal nature of the current by considering its sensitivity to scattering. In multiterminal setups, we reveal the characteristic phase dependences of the supercurrents explaining those in terms of interference of Andreev reflection processes. For more complex setups encompassing, at least, two constrictions, we find an interplay between noninteracting and interaction-induced currents and contributions of more complex interference processes.

## I. INTRODUCTION

Topological edge states, from their first discovery in quantum Hall systems [1] through the advent of topological insulators [2], have proved to be both interesting by themselves [3–5] as well as a tool for fundamental physics research and practical applications [6]. Their chirality/helicity and the quantized conductance have all played their own important roles. It is feasible and interesting to combine quantum Hall physics with superconductivity by contacting the edge channels with superconducting electrodes; this being a subject of intensive theoretical and experimental research [7–12].

The quantum Hall systems can be devised to arrange the scattering between the edge channels of different chirality by making corner junctions or constrictions. In Refs. [13–15], the authors studied the interferometers made from corner junctions between edge channels for integral and fractional quantum Hall systems. In Ref. [16], they have examined tunneling between edge states via an intermediate quantum Hall island. In Ref. [17], the authors have proposed to use a tunnel junction to probe the helicity of edge states. Such quantum Hall setups can be combined with superconducting electrodes [12]. Beenakker [18] has proposed an experimental setup for probing annihilation probability between Bogoliubov quasiparticles from two superconducting sources with a phase difference between them with the goal to demonstrate their Majorana nature. The quantum Hall setups may include more than two superconducting electrodes, such multiterminal superconducting structures are under active theoretical and experimental investigation [19–25].

Recently, the authors have addressed the supercurrents in a long chiral integer Hall edge channel with two superconducting electrodes [26]. Although this current vanishes in approximation of noninteracting electrons, we have shown the possibility of an interaction-induced supercurrent. This supercurrent appeared to require a nonlocal electron-electron interaction and is related to an information flow in the direction opposite to the electron flow that is provided by such interaction. We have considered several specific interaction models and formulated an external circuit model that facilitates controllable and efficient nonlocal interaction.

In this article, we study the specific features of the phenomenon in order to facilitate its experimental verification. We show that the dynamical phase that may be induced by electrostatic potential affects the superconducting interference in sharp contrast with the nonchiral systems. We consider more complex quantum Hall setups that involve scattering between the edge channels and multiple superconducting electrodes and compute the interaction-induced supercurrent in these setups. This is important in view of the fact that the setups are easy to employ and flexible to reveal the peculiarities of the effect under consideration. To avoid unnecessary details, we consider only a simplest external circuit model of the nonlocal interaction. Qualitatively, the results hold for any other nonlocal interaction.

In all setups, the supercurrent values are of the same order of magnitude as for the single channel case but do depend on details of potential and Andreev scattering in the structure. Full and general analysis can be performed in a situation of a single constriction where the electron trajectories do not make loops. We specify to several distinct setups, some demonstrating the nonlocal nature of the interaction-induced

supercurrent, some, such as the Beenakker setup, not exhibiting any supercurrent at all.

In a similar fashion, we analyze the supercurrents for the case of many superconducting terminals connected to a single edge channel. We reveal the relation between the current and a complex amplitude of Andreev scattering that is contributed by a multitude of partial amplitudes corresponding to various sequences of Andreev processes. For two superconducting electrodes, the phase dependence of the current is sinusoidal suggesting single Cooper pair transfers as the dominant transport mechanism. More electrodes complicate this dependence that gives the signatures of multiple Cooper pair transfers.

As an example of more complex and potentially interesting situation, we consider a setup comprising two constrictions and two or three superconducting electrodes. The presence of loop trajectories complicates the sequences of Andreev processes and may lead to an interplay of interaction-induced and common proximity supercurrents that results in a complicated phase dependence of the current.

The paper is organized as follows. In Sec. II, we recite the previous results on interaction-induced supercurrent, explain the model, and the way to derive the effect microscopically. We also consider the effect of dynamical phase. In Sec. III, we apply these concepts to a single junction setup, derive a general formula, and specify it to a variety of the situations. In Sec. IV, we discuss the supercurrents in multiple superconducting terminals connected to a single edge channel. In Sec. V, we consider a more complex setup comprising two constrictions and three superconducting terminals. We conclude in Sec. VI.

## II. INTERACTION-INDUCED SUPERCURRENT IN QUANTUM HALL EDGE CHANNELS

Here, we introduce the microscopic model, shortly recite the results of Ref. [26], and explain the mechanism of the interaction-induced supercurrent.

Let us consider a chiral channel at the edge of a quantum Hall bar (Fig. 1). We assume that the relevant energy scales are much smaller than the Landau-level separation, thus, the edge states can be described with a Hamiltonian encompassing electron field operators $\psi_\sigma(x)$ with a linear spectrum near Fermi level, $\sigma = \uparrow, \downarrow$ being the spin index,

$$H_0 = -iv_F \sum_\sigma \int dx\, \psi_\sigma^\dagger(x)\partial_x \psi_\sigma(x). \quad (1)$$

In addition to this, we include the terms with the electrostatic potential $V(x)$ and the pairing potential $\Delta(x)$ induced to the channel in the vicinity of superconducting electrodes,

$$H_1 = \sum_\sigma \int dx\, V(x)\psi_\sigma^\dagger(x)\partial_x \psi_\sigma(x)$$

$$+ \int dx[\Delta^*(x)\psi_\uparrow(x)\psi_\downarrow(x) + \Delta(x)\psi_\downarrow^\dagger(x)\psi_\uparrow^\dagger(x)]. \quad (2)$$

We have not considered the electrostatic potential in Ref. [26].
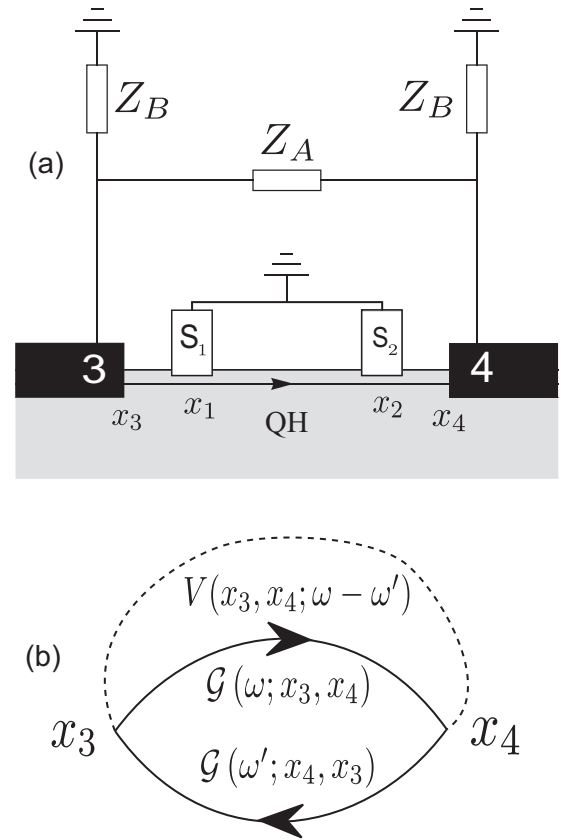


FIG. 1. Interaction-induced supercurrent in a quantum Hall edge (QHE) channel. (a) A chiral channel at the edge of the quantum Hall bar (light gray) is connected to two superconducting electrodes in the points $x_{1,2}$. Further away, the channel is covered with metallic electrodes 3 and 4 that provide a nonlocal electron-electron interaction between points $x_{3,4}$. (b) The diagram for the relevant interaction correction to the total energy of the system, $\mathcal{G}$ being electron Green's functions, and $V$ being the interaction. The chirality of the channel requires that the diagram gives a nonzero contribution only if $\omega\omega' < 0$.

The resulting Matsubara Green's function $\mathcal{G}(\omega; x, x')$ is a $2 \times 2$ matrix in Nambu space and satisfies

$$[-i\omega - iv_F\partial_x + \mathcal{H}(x)]\mathcal{G}(\omega; x, x') = -\delta(x - x'), \quad (3)$$

$$\mathcal{H}(x) = V(x)\tau_z + \Delta(x)\tau^+ + \Delta^*(x)\tau^-, \quad (4)$$

where $\tau_z, \tau^\pm = (\tau_x \pm i\tau_y)/2$ are Pauli matrices in Nambu space.

It is important to note that the chirality of the channel is manifested in the form of Green's functions as follows: $\mathcal{G}(\omega; x, x') = 0$ if $\omega > 0$, $x > x'$ or $\omega < 0$, $x < x'$. We compute the supercurrent as a part of the energy that depends on the difference of the superconducting phases. For this correction, the Green's functions should form a closed loop encompassing the coordinates of the superconducting terminals $x_{1,2}$. The above property makes such a loop equal to zero if the Green's functions are at the same energy $\omega$. This forbids the supercurrent for noninteracting electrons. Such a loop is, however, not zero if the frequencies of the Green's functions making the loop are opposite in sign; this may be

the case when they are the parts of the interaction correction [Fig. 1(b), the loop is formed if $\omega\omega' < 0$]. The interaction that leads to supercurrent must be a nonlocal one: Since the loop encompasses $x_1, x_2$, the interaction line should connect the points $< x_1$ to those $> x_2$.

The general form of the interaction correction reads

$$(\Delta E) = -2 \int d\omega\, d\omega'\, dx\, dx'\, V(\omega - \omega'; x, x)$$
$$\times \text{Tr}[\mathcal{G}(\omega; x, x')\hat{\tau}_z \mathcal{G}(\omega'; x', x)\hat{\tau}_z]. \quad (5)$$

Let us elaborate on the Green's functions. Since those obey the first-order differential equation, its general solution for $\omega > 0$ reads

$$v_F \mathcal{G}(\omega; x, x') = \exp\left[-\frac{\omega(x - x')}{v_F}\right] P \exp\left[-\frac{i}{v_F} \int_x^{x'} dz\, \mathcal{H}(z)\right] \quad (6)$$

where $P$ indicates the position ordering of the exponent arguments that are arranged from the left to the right in descending order of their coordinates.

The contributions of pairing and electrostatic potential to the position-ordered exponent are separated in space differently. The contributions of $\Delta$ come from the vicinity of each superconducting lead $i$,

$$\hat{U}_i = P \exp\left(-iv_F^{-1} \int dz[\Delta(z)\tau^+ + \Delta^*(z)\tau^-]\right), \quad (7)$$

where the integration interval covers the vicinity and are readily expressed in terms of the electron-hole conversion (Andreev) probability $p_i$ at this lead,

$$U_i = \begin{pmatrix} \sqrt{1 - p_i} & -ie^{i\phi_i}\sqrt{p_i} \\ -ie^{-i\phi_i}\sqrt{p_i} & \sqrt{1 - p_i} \end{pmatrix}. \quad (8)$$

It is a unitary matrix that depends on the superconducting phase $\phi_i$ at this particular lead. The contribution of the electrostatic potential is accumulated on an interval $x_b > x_a$ and reads

$$\hat{K}_{ab} = \begin{pmatrix} e^{i\chi_{ab}} & 0 \\ 0 & e^{-i\chi_{ab}} \end{pmatrix}, \quad \chi_{ab} = -\int_{x_a}^{x_b} dx\, V(x)/v_F, \quad (9)$$

$\chi_{ab}$ being a dynamical phase [27] accumulated over the interval. With this, for any interval $(x_3, x_4)$ that includes the superconducting electrodes, the Green's function reads

$$v_F \mathcal{G}(\omega; x_3, x_4) = -e^{-(\omega/v_F)(x_3 - x_4)}[\theta(\omega)\theta(x_3 - x_4)\hat{Q} - \theta(-\omega)\theta(x_4 - x_3)\hat{Q}^{-1}], \quad (10)$$

where a unitary matrix $\hat{Q}$ is the $P$-ordered exponent on this interval,

$$\hat{Q} = \hat{K}_{31}\hat{U}_1\hat{K}_{12}\hat{U}_2\hat{K}_{24}. \quad (11)$$

The energy correction contains a factor incorporating information about the Andreev reflection and superconducting phases,

$$A = \text{Tr}[\hat{Q}\tau_z\hat{Q}^{-1}\tau_z]. \quad (12)$$

Since the matrices on the ends $\hat{K}_{31}, \hat{K}_{24}$ commute with $\tau_z$, we can neglect those and reduce $Q$ to $Q' \equiv \hat{U}_1\hat{K}_{12}\hat{U}_2$. With this,

$$A = 2(1 - 2p_1)(1 - 2p_2) - 8\sqrt{p_1(1 - p_1)p_2(1 - p_2)}$$
$$\times \cos(\phi_1 - \phi_2 - 2\chi_{21}). \quad (13)$$

Let us specify the interaction to the model used in Ref. [26]. To realize a nonlocal interaction that transfers the electric signals upstream, one embeds the QHE edge into an external electric circuit [Fig. 1(a)]. To connect the edge to the circuit, we cover it with two metallic electrodes that are spread at $x < x_3$ and $x > x_4$, respectively ($x_4 - x_3 \equiv \tilde{L}$). By a gauge transform, the interaction can be reduced to the contact points and is expressed in terms of the cross impedance between these electrodes [for the circuit in Fig. 1(a), $Z_{34} = Z_B^2/(Z_A + 2Z_B)$],

$$V(\nu; x, x') = \frac{v_F^2}{2}\delta(x - x_3)\delta(x - x_4)\frac{Z_{34}(\nu)}{|\nu|}. \quad (14)$$

We stress that the interaction in question is an environment-induced interaction *between* the quasiparticles rather than an interaction of a quasiparticle with the environment of the external circuit. The latter can provide decoherence and dissipation but not the effect under consideration. It is also clear from the fact that this interaction is proportional to a cross impedance between the distant parts of the edge channel.

We specify to the model of the frequency-independent (at the scale $\simeq v_F/\tilde{L}$) impedance to arrive at

$$\Delta E = \frac{A R_{34}}{2}; \quad R_{34} = \frac{e^2}{\pi^2}\frac{v_F}{\tilde{L}}Z_{34}. \quad (15)$$

We compute the current by differentiating the energy with respect to the phase difference $\phi \equiv \phi_1 - \phi_2$,

$$I(\phi) = 2\partial_\phi(\Delta E)$$
$$= -8eR_{34}\sqrt{p_1 p_2(1 - p_1)(1 - p_2)}\sin(\phi - 2\chi_{21}). \quad (16)$$

This differs from the answer given in Ref. [26] by the inclusion of the dynamical phase $\chi_{21}$ that effectively shifts the superconducting phase difference. The dynamical phase is invariant with respect to time reversal whereas the superconducting phase is not, so one may wonder why those two match each other. However, the time reversibility is essentially violated in QHE regime, and the chirality sets the relation between the phases. This leads to interesting and measurable consequences: The supercurrent between two electrodes can be modulated by a gate voltage applied to the channel to induce the dynamical phase. This effect of the gate voltage is rather local: It needs to be applied to the part of the channel between the superconducting electrodes.

The scale of the current is $e$ times the inverse time of flight between the electrodes $v_F/\tilde{L}$ times a small factor that is the dimensionless impedance $Z_{34}e^2/\hbar$. A common estimation of for $Z_{34}$ is the vacuum impedance, this gives the small factor $\simeq 10^{-2}$.

Let us note that the current is a sinusoidal function of phase. In usual nonchiral superconducting junctions, this occurs only in the limit of low transparency, and the corresponding process is identified as a single Cooper pair tunneling between electrodes 1 and 2. Here, the transparency is high since the channel is completely ballistic. Nevertheless, the
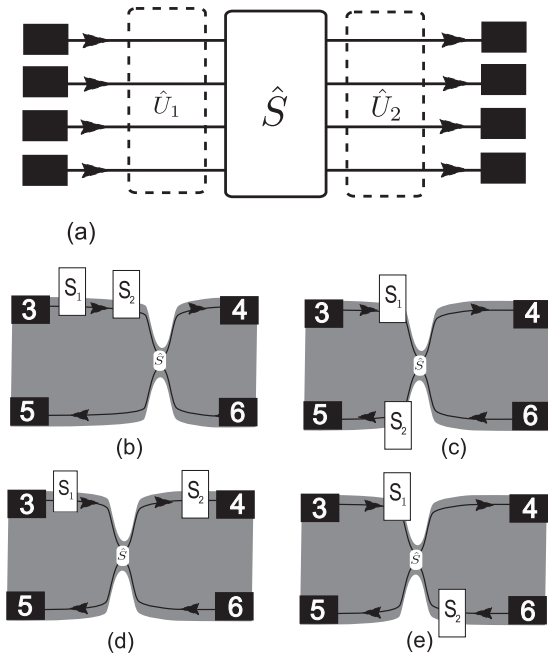
FIG. 2. Single constriction setups. (a) General framework for all possible single-constriction setups. We count the coordinates for each channel from the constriction in the direction of the channel propagation. In this way, we can describe Andreev and potential scatterings on the same footing with a local potential that may mix $N$-propagating channels. This allows for an easy generalization of the single-channel approach. (b)–(e) Various setups. The modulation of the constriction transmission changes the interaction coefficient in the setup (b) and propagation probability in the setups (d) and (c). No interaction-induced supercurrent is found in setup (e).

underlying elementary process seems to be a single Cooper pair tunneling. Thus, the sinusoidal dependence requires a separate explanation.

In fact, the prefactor $A$ given by Eq. (12) contains the probability of Andreev conversion (from the electron to the hole or vice versa) of a quasiparticle that passes the structure. The elementary process responsible for the supercurrent is, thus, an Andreev conversion of a single quasiparticle upon its transfer in the direction of the flow. The conversion may occur in either of the two electrodes, and the supercurrent comes about from the interference of these two possibilities. The dependence is sinusoidal since, for the two-electrode setup, there can be only a *single* conversion. As we will see in Sec. IV, more conversions can occur in the setups with more superconducting electrodes, and this results in higher harmonics in the phase dependence of the current.

## III. SINGLE CONSTRICTION

The simplest way to make a nontrivial QH setup is to make a constriction in a QH bar with the width that is comparable with the spread of the edge channel wave functions [Figs. 2(b)–2(e)]. There is a scattering of the electron waves at the constriction: Upon passing the constriction, an incoming electron will either stay at the same edge with probability $T$ or be reflected to the opposite edge with probability $1 - T$. In all

setups, we implement the external circuit nonlocal interaction: The beginning and end of each channel is covered by a metal electrode included in the circuit (not shown in the figure).

A common specific feature of all single-constriction setups is that the electron trajectories do not form any closed loops whatever the scattering they experience. This is why all such setups can be treated in the same manner. We do this by counting the coordinates for each channel separately in the direction of propagation, starting form a point in the constriction. In this way, we can reduce all setups to a single general model depicted in Fig. 2(a). There, we have $N$-chiral channels subject to local pairing and electrostatic potential, these potentials being $N \times N$ matrices in the channel space. The Green's function is also a matrix in channel space satisfying

$$[-i\omega - i\check{v}_F \partial_x + \mathcal{H}(x)]\mathcal{G}(\omega; x, x') = -\check{\mathbb{1}}\delta(x - x'), \quad (17)$$

$$\mathcal{H}(x) = \check{V}(x)\tau_z + \check{\Delta}(x)\tau^+ + \check{\Delta}^*(x)\tau^-, \quad (18)$$

where "check" denotes the matrix structure in the channel space. We note that $v_F$ also has this structure since the velocity may depend on the channel. Apart from this extra structure, the Eq. (17) is a complete analog of Eq. (3) and can be solved with a position-ordered exponent.

To simplify further, we note that the pairing potential is diagonal in channels either before or after the constriction, and the nondiagonal potential is localized on the constriction [Fig. 2(a)]. With this, the Green's function can be represented in a form analogous to Eq. (10), $a$, $b$ being the channel indices and $x$, $x'$ are beyond the scattering region,

$$\sqrt{v_F^a v_F^b}\mathcal{G}^{ab}(\omega; x, x') = -e^{[-(|\omega|/v_F)|x-x'|]}[\theta(\omega)\theta(x - x')\hat{Q}^{ab}$$
$$- \theta(-\omega)\theta(x' - x)(\hat{Q}^{-1})^{ab}]. \quad (19)$$

The unitary matrix $\hat{Q}$ is composed of the matrices of the superconducting electrodes before and after the constriction, and the matrix $\hat{S}$ that describes the scattering at the constriction,

$$\hat{Q} = \hat{U}_1\hat{S}\hat{U}_2. \quad (20)$$

For two channels,

$$\hat{S} = \check{s}\frac{1 + \tau_z}{2} + \check{s}^\dagger\frac{1 - \tau_z}{2}, \quad \check{s} \equiv \begin{pmatrix} t & r \\ -r' & t' \end{pmatrix}. \quad (21)$$

$t$, $t'$ and $r$, $r'$ being the transmission and reflection amplitudes at the constriction. To compute the interaction correction, we employ the external circuit nonlocal interaction model. In general, we have the contributions from each pair of the electrodes at the beginning and at the end of the channel, those are weighted with the corresponding cross impedances.

We are ready to derive the answers for the specific setups. Let us start with one shown in Fig. 2(b). Here, both superconducting electrodes are connected to the same channel upstream from the constriction. Naively, one would regard the superconducting current as a local quantity determined by the electrodes and the space between those. However, this is not true in view of the nonlocal character of the interaction. The setup provides a good and practical illustration for this. Similar to Eq. (16), the current is given by
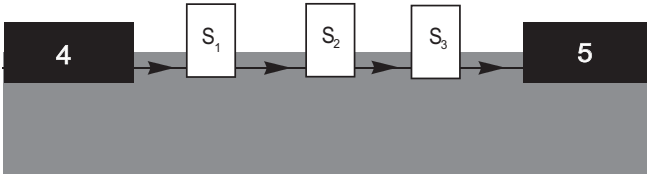
FIG. 3. Multiple superconducting electrodes contacting the same channel $N = 3$.

$$I = -8eR_B\sqrt{p_1p_2(1-p_1)(1-p_2)}\sin(\phi - 2\chi_{21}) \text{ with}$$

$$R_B = \frac{e^2}{\pi^2}\left(T\frac{v_F}{L_3+L_4}Z_{34} + (1-T)\frac{v_F}{L_3+L_5}Z_{35}\right). \quad (22)$$

Here, and further in the text, $L_i$ is the distance from the constriction to the metallic electrode $i$. We see that the interaction coefficient $R$ does depend on the transmission of a distant constriction switching between two values corresponding to completely open and closed constriction. A gate that modulates this transmission will modulate this interaction coefficient and current without changing the external circuit. This would be a convenient experimental proof of nonlocality. A similar result is obtained if both electrodes connect the same channel downstream the constriction.

If one electrode is upstream from the constriction, and another one is downstream [Figs. 2(c) and 2(d)], the modulation of the transmission modifies the probability to go from one to another rather than the interaction. The current is given by $I = -8eR_{C,D}\sqrt{p_1p_2(1-p_1)(1-p_2)}\sin(\phi - 2\chi_{21})$ with

$$R_C = \frac{e^2}{\pi^2}(1-T)\frac{v_F}{L_3+L_5}Z_{35}, \quad R_D = \frac{e^2}{\pi^2}T\frac{v_F}{L_3+L_4}Z_{34}. \quad (23)$$

The dynamical phase $\chi_{21}$ is accumulated along a path passing the constriction and eventually incorporates the phase of either transmission or reflection amplitude. Interestingly, $R_B = R_C + R_D$, and this can be used for the experimental identification of the effect.

For a setup where the superconducting electrodes are either upstream or downstream from the constriction but contact different channels [Fig. 2(e)], we find no interaction-induced supercurrent. This is related to the fact that a closed loop of Green's functions encompassing both electrodes always equals zero. Beenakker [18] has proposed to measure current noise correlations in the setup. Luckily, those would not be obscured by the supercurrent.

## IV. MULTIPLE SUPERCONDUCTING TERMINALS

In view of a significant experimental and theoretical interest to multiterminal superconducting nanostructures, we consider here multiple superconducting electrodes connected to the same channel. The approach outlined in the previous section suits for multiple superconducting electrodes as well. Here, we concentrate on a simple but general situation when $N$-superconducting electrodes are in contact with the same channel (Fig. 3 gives the setup for $N = 3$).

The Green's function between the edges of metallic electrodes is given by Eq. (10) with $Q$ encompassing all matrices $\hat{U}_i$, $i = 1 \cdots N$ of the superconducting electrodes and the matrices $\hat{K}_{i,i+1}$ responsible for the accumulation of dynamical phase between the electrodes,

$$\hat{Q} = \prod_{i=1}^{N-1}\hat{U}_i\hat{K}_{i,i+1}\hat{U}_N. \quad (24)$$

Here, we skip $\hat{K}$ matrices before and after the superconducting electrodes since they do not affect the answer for the current.

The energy correction is given by $\Delta E = AR/2$ where the interaction coefficient $R$ is defined by the interaction via the external circuit,

$$R = \frac{e^2}{\pi^2}\frac{v_F}{\tilde{L}}Z_{45}, \quad (25)$$

whereas

$$A = 2(1 - 2|Q_{eh}|^2) \quad (26)$$

incorporates all the information about the Andreev probabilities and superconducting phases.

Actually, $Q_{eh}$ is the amplitude of Andreev conversion of an electron to a hole while passing the setup, and $|Q_{eh}|^2$ is the conversion probability. It is instructive to regard it as a sum of partial Andreev amplitudes corresponding to different sequences of conversion or passing at the electrodes. For instance, there are partial amplitudes where the electron is converted at one of the electrodes passing all other. Another set of the partial amplitudes corresponds to the case when the electron is converted to the hole at the first electrode, the hole is converted back to the electron at the second, and finally back to hole at the third one, whereas passing all others. Each partial amplitude, in agreement with Eq. (24), is a product of amplitudes from all electrodes and spaces in between those. Let us give an example of such analysis for $N = 3$ and derive the expression for $A$.

The amplitude of the process where the conversion occurs at electrode 1 reads

$$\mathcal{A}_1 = -i\sqrt{p_1}\sqrt{1-p_2}\sqrt{1-p_3}e^{i\phi_1}e^{-i\chi_{12}}e^{-i\chi_{23}}, \quad (27)$$

similar contributions for electrodes 2 and 3 are obtained by index exchange and change in signs of the dynamical phase,

$$\mathcal{A}_2 = -i\sqrt{p_2}\sqrt{1-p_1}\sqrt{1-p_3}e^{i\phi_2}e^{i\chi_{12}}e^{-i\chi_{23}}, \quad (28)$$

$$\mathcal{A}_3 = -i\sqrt{p_3}\sqrt{1-p_2}\sqrt{1-p_1}e^{i\phi_3}e^{i\chi_{12}}e^{i\chi_{23}}, \quad (29)$$

and there is a contribution that corresponds to the conversion at each electrode,

$$\mathcal{A}_{123} = (-i)^3\sqrt{p_1}\sqrt{p_2}\sqrt{p_3}e^{i\phi_1}e^{-i\chi_{12}}e^{-i\phi_2}e^{i\chi_{23}}e^{i\phi_3}. \quad (30)$$

Let us, for convenience, shift the phases $\phi_{1,3}$ with the corresponding dynamical phases $\phi_1 \rightarrow \phi_1 - 2\chi_{12}$, $\phi_3 \rightarrow \phi_3 + 2\chi_{23}$. With this, we express the conversion probability as

$$|Q_{eh}|^2 = p_2(1-p_1)(1-p_3) + p_1(1-p_2)(1-p_3)$$

$$+ p_3(1-p_2)(1-p_1) + p_1p_2p_3 \quad (31)$$

$$+ 2\sqrt{p_1(1-p_1)p_2(1-p_2)}\cos(\phi_1 - \phi_2) \quad (32)$$

$$+ 2\sqrt{p_2(1-p_2)p_3(1-p_3)}\cos(\phi_2 - \phi_3) \quad (33)$$

$$+ 2\sqrt{p_1(1-p_1)p_3(1-p_3)}(1-p_2)\cos(\phi_1 - \phi_3) \quad (34)$$

$$- 2\sqrt{p_1(1-p_1)p_3(1-p_3)}p_2\cos(2\phi_2 - \phi_3 - \phi_1). \quad (35)$$

Here, the term (31) comprises the squares of the partial amplitudes. It does not depend on phases and, therefore, does not contribute to the current. The term (32) comes about the interference of the amplitudes in pairs $\mathcal{A}_1$, $\mathcal{A}_2$ and $\mathcal{A}_3$, $\mathcal{A}_{123}$. Somewhat surprisingly, it corresponds to the currents between electrodes 1 and 2 as if the third electrode was not at all present. The same applies to the term (33): It corresponds to the current between electrodes 2 and 3 as if no electrode 1 is present and arises from the interference of the amplitudes in pairs $\mathcal{A}_3$, $\mathcal{A}_2$ and $\mathcal{A}_1$, $\mathcal{A}_{123}$. The term (34) describes the current between 1 and 3 only, although its amplitude is reduced by Andreev conversion at electrode 2 and manifests interference between $\mathcal{A}_1$ and $\mathcal{A}_3$. All these terms lead to the currents as if there were tunnel junctions connecting the corresponding electrodes and manifest a single Cooper pair tunneling between the electrodes. The last term (35) is of a different nature. It manifests a more interesting process of two Cooper pair tunnelings: The Cooper pairs from 1 and 3 simultaneously entering electrode 2, or reversely, two Cooper pairs from 2 getting to 1 and 3 that cannot be described with elementary tunnel junctions. For a bigger number of electrodes, more complex processes, involving more electrodes and Cooper pairs, are manifested.

Finally, the currents read (we count the phases from electrode 2, $\phi_2 = 0$),

$$I_1 = I_1^0 \sin \phi_1 + I_{13} \sin(\phi_1 - \phi_3) + I_i \sin(\phi_1 + \phi_3), \quad (36)$$

$$I_3 = I_3^0 \sin \phi_1 + I_{13} \sin(\phi_3 - \phi_1) + I_i \sin(\phi_1 + \phi_3), \quad (37)$$

$I_2 = -I_3 - I_1$, where $I_i^0 = -8eR_{45}\sqrt{p_i p_2 (1 - p_i)(1 - p_2)}$, $I_{13} = -8eR_{45}\sqrt{p_1 p_3 (1 - p_1)(1 - p_3)(1 - p_2)}$, $I_i = -8eR_{45}$ $\sqrt{p_1 p_3 (1 - p_1)(1 - p_3)}p_2$. The last terms $\propto I_i$ are due to the interesting process. The currents are shifted sinusoidal functions of any phase.

## V. AN EXAMPLE OF A COMPLEX SETUP

It is not difficult to form two constrictions in a Hall bar (Fig. 4). This provides an example of a more complex setup that cannot be understood with the approach of the previous sections. The reason for this is a possibility of looping electron trajectories that provide multiple Andreev conversions from the same electrodes multiple scatterings at the same constric-
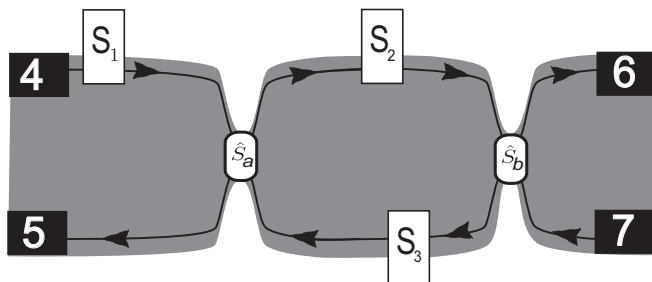


FIG. 4. An example of a more complex setup: A Hall bar with two constrictions. This provides a possibility of electron trajectories that loop over the ring between the constrictions $a$ and $b$. This leads to noninteracting current between electrodes 2 and 3. The supercurrent to 1 is interaction induced and is evaluated in this section.

tion. In the setup under investigation, the loops occur in the ring between constrictions $a$ and $b$.

It has to be noted that looping trajectories lead to a non-interacting current, in this case, between electrodes 2 and 3. The magnitude of this current can be estimated as $ev_F/L_c$ and is typically much bigger than the expected interaction-induced current. The precise expression can be derived from the phase-dependent contribution to the ground-state energy that reads

$$\Delta E = -\frac{v_F}{L_c} \sum_{pm} \mathrm{Li}_2(\sqrt{R_a R_b} e^{\pm i\lambda}). \quad (38)$$

Here, $\mathrm{Li}_2$ is the dilogarithm function, $e^{\pm i\lambda}$ are the eigenvalues of the matrix $\hat{Q}_c = \hat{U}_2 \hat{K}_{23} \hat{U}_3 \hat{K}_3 2$, the matrices $\hat{U}_{2,3}$ represent Andreev conversion at the corresponding electrodes whereas $\hat{K}_{23,32}$ represent the accumulation of dynamical phases on paths $2 \to 3$, $3 \to 2$ and include the phases of the reflection amplitudes $r_a$, $r_b'$, respectively. More explicitly,

$$\cos \lambda = Q_0$$
$$= \cos(\chi_{23} + \chi_{32})\sqrt{(1 - p_2)(1 - p_3)}$$
$$+ \sqrt{p_2 p_3} \cos(\phi_2 - \phi_3 + \chi_{32} - \chi_{23}). \quad (39)$$

However, the supercurrent from electrode 1 can only be due to a nonlocal interaction. Let us compute the contribution proportional to $Z_{45}$; all other contributions can be evaluated in the same manner. We start with evaluation of $\mathcal{G}(\omega, x_4, x_5)$ at $\omega > 0$. It is determined by electron-hole propagation between these points and is a sum of partial propagation amplitudes with a different number of loops in the ring between constrictions $a$ and $b$. The contribution with no loops encompasses the propagation along the paths $4 \to a \to 5$ and reads

$$\mathcal{G}^{(0)} = e^{-[\omega(L_4 + L_5)/v_F]} \hat{U}_1 \hat{r}_a. \quad (40)$$

Here, to shorten the notations, we introduce $\hat{\tilde{U}}$ that incorporates the adjacent $\hat{K}$ (for instance, $\hat{\tilde{U}}_1 = \hat{K}_{51} \hat{U}_1 \hat{K}_{1a}$) skip the irrelevant $\hat{K}$ at the end of the path. The contribution with one loop, in addition to this, encompasses the path $a \to 2 \to b \to 3 \to a$,

$$\mathcal{G}^{(1)} = e^{-[\omega(L_4 + L_5)/v_F]} \hat{\tilde{U}}_1 \hat{t}_a e^{-(\omega L_c/v_F)} \hat{\tilde{U}}_2 \hat{r}_b \hat{\tilde{U}}_2. \quad (41)$$

The contributions with higher loop numbers form a geometric series where each term is multiplied with $\hat{r}_a' \hat{\tilde{U}}_2 \hat{r}_b \hat{\tilde{U}}_3 \exp(-\omega L_c/v_F) \equiv \hat{Q}_c \sqrt{R_a R_b} \exp(-\omega L_c/v_F)$. This sums up to

$$\mathcal{G} = e^{-[\omega(L_4 + L_5)/v_F]} \hat{\tilde{U}}_1 \{\hat{r}_a + [\hat{t}_a (\hat{r}_a')^{-1} \hat{M} \hat{t}_a']\}, \quad (42)$$

$$\hat{M} \equiv \frac{\hat{Q}_c \sqrt{R_a R_b} e^{-(\omega L_c/v_F)}}{1 - \hat{Q}_c \sqrt{R_a R_b} e^{-(\omega L_c/v_F)}}. \quad (43)$$

We concatenate this with another Green's function at $\omega'$ and integrate over $\omega, \omega'$. This integration is more involved than in the previous cases since the propagation involves the paths of different lengths $L = L_4 + L_5 + nL_c$, $n$ being the number of the loops made by a trajectory. The answer involves many different combinations of dynamical phases.

To simplify, we shift $\phi_2 \to \phi_2 + \mu + \nu$, $\phi_3 \to \phi_3 + \mu - \nu$, $\mu \equiv \arg(r'_a) + \chi_{a2}$, $\nu \equiv \chi_{2b} + \arg(r_b) + \chi_{b3}$ and introduce

$$\chi_A = 2\chi_{1a} + \arg(t_a) - \arg(r'_a) - \arg(t'_a) - \chi_{3a}, \quad (44)$$

$$\chi_B = 2\chi_{1a} + 2\arg(t_a) - 2\arg(r'_a) + \nu + \mu, \quad (45)$$

$$\chi_C = 2\chi_{1a} + 2\arg(t_a) - 2\arg(r'_a) - \chi_{3a}. \quad (46)$$

With this,

$$\Delta E = -4\sqrt{p_1(1-p_1)}T_a \frac{e^2}{\pi^2} \frac{v_F}{L_4 + L_5} Z_{34}$$

$$\times \left\{ \sqrt{R_a R_b} \mathcal{F}_A [\cos(\chi_A - \phi_1 + \phi_2)\sqrt{p_2(1-p_3)} \right. \quad (47)$$

$$+ \cos(\chi_A - \phi_1 + \phi_3)\sqrt{p_3(1-p_2)}] \quad (48)$$

$$+ 2T_a R_b \mathcal{F}_B [-\cos(\chi_B - \phi_1 + \phi_2)\sqrt{p_2(1-p_2)}(1-p_3)$$

$$- \cos(\chi_B - \phi_1 + \phi_3)\sqrt{p_3(1-p_3)}(1-p_2)$$

$$+ \cos(\chi_B - \phi_1 - \phi_3 + 2\phi_2)\sqrt{p_3(1-p_3)}p_2] \quad (49)$$

$$+ T_a R_b^{3/2} R_a^{1/2} \mathcal{F}_C [\cos(\chi_C - \phi_1 + \phi_2)\sqrt{p_2(1-p_3)}$$

$$\left. + \cos(\chi_C - \phi_1 + \phi_3)\sqrt{p_3(1-p_2)}] \right\}. \quad (50)$$

Here, the dimensionless coefficients $\mathcal{F}_{A,B,C}$ come about the frequency integration. They depend on the ratio of paths $c \equiv L_c/(L_4 + L_5)$, the reflection coefficient $\sqrt{R_A R_B}$ in the ring, and incorporate information about the Andreev conversion, superconducting, and dynamical phases in the ring by a single parameter $Q_0$ defined by Eq. (39).

The coefficients are expressed in integral form as

$$\mathcal{F}_A = \int_0^\infty \frac{dx\, dx'}{x + x'} e^{-(x+x')} [e^{-cx}D(x) + e^{-cx'}D(x')], \quad (51)$$

$$\mathcal{F}_B = \int_0^\infty \frac{dx\, dx'}{x + x'} e^{-(x+x')(1+c)}D(x)D(x'); \quad (52)$$

$$\mathcal{F}_B = -\int_0^\infty \frac{dx\, dx'}{x + x'} e^{-(x+x')(1+c)}(e^{-cx'} + e^{-cx})D(x)D(x'); \quad (53)$$

$$D^{-1}(x) = 1 - 2\sqrt{R_a R_b}Q_0 e^{-cx} + R_a R_b e^{-2cx}. \quad (54)$$

They approach constant limits at $c \to 0$ and scale as $1/c$ at $c \to \infty$; this signifies that in the limit of large ring circumferences the energy scale is determined by $L_c$.

Let us consider and interpret the terms in the phase-dependent energy correction. We see that the overall expression is proportional to $T_a$ since the electrons should get to the ring to feel other superconducting ring. The terms (48) proportional to $\mathcal{F}_A$ come about the interference of paths that do and do not visit the ring, and this is seen from square-root dependence on the reflection coefficients. We have not encountered this situation in the previous sections since there any relevant path passes all the electrodes. We see this in different dependences of the coefficients on Andreev conversion probabilities, for instance, $\sqrt{p_2(1-p_3)}$ misses the factor $\sqrt{1-p_2}$ present in the previous expressions. The phase dependence of the terms can be still interpreted in terms of

single Cooper pair tunneling between either 1 and 2 or 1 and 3.

The terms (49) proportional to $\mathcal{F}_B$ arise from the interference of various trajectories that visit the ring and experience Andreev conversion when going from 4 to 5. Their structure is similar to that studied in the previous section. There is a term that manifests a process whereby two Cooper pairs from 1 and 3 enter electrode 2. It has to be present since in the limits $R_b \to 1$, $R_a \to 0$ we return to the single-channel setup considered in Sec. IV where the two-Cooper pair tunneling has been identified. The terms (50) proportional to $\mathcal{F}_C$ result from the interference of the trajectories that pass the ring with and without Andreev conversion in the ring. This is why the dependence of the coefficients on the conversion probabilities is identical to that of (48). The presence of looping trajectories and various paths leads to the fact that the similar terms pick up different dynamical phases that cannot be compensated with the shifts of the superconducting phases as in the previous examples.

## VI. CONCLUSIONS

In conclusion, we have extended the previous study of interaction-induced supercurrents in a single quantum Hall edge channels to experimentally relevant and widely used quantum Hall setups with scattering between the edge channels. We restricted ourselves to a simple but relevant interaction model where the informational flow in the direction opposite to that of the electron propagation is provided by an external circuit.

For a single constriction in a Hall bar, the considerations are simple and can be performed in very general form. We have considered specific setups that manifest the nonlocal nature of the interaction-induced effect whereby a supercurrent can be modulated by changing the transmission coefficient of a distant constriction. We have considered a multiterminal superconducting system where the electrodes are connected to a single edge channel, understood the supercurrent in terms of interference of Andreev conversion processes, and have identified a process that can be regarded as two-Cooper pair tunneling.

We have considered a more complex exemplary setup that involves two constrictions and thereby gives a possibility of looping trajectories. This gives rise to interplay of noninteracting and interaction-induced currents and significantly complicates the situation. We demonstrate the evaluation of the phase-dependent energy correction in this complex setup and interpret the result in terms of various interference processes.

The results presented facilitate the experimental observation of interaction-induced supercurrent and contribute to the active field of superconductor-QHE nanostructures. The most interesting experimental signatures revealed in this article include: (i) The effect of dynamical phase (induced by a gate electrode) on the superconducting interference that is the signature of chirality; (ii) the absence or presence of the effect depending on the positioning of superconducting electrodes with respect to the constriction (Fig. 2). In particular, we prove that the Beenakker setup is not affected by the interaction-induced supercurrent. (iii) Modulation of the current by modulation of the transparency of the constriction

the current does not go through: a striking manifestation of the essentially nonlocal nature of the interaction-induced supercurrent (Sec. III); (iv) subsequent interaction-induced Andreev reflection in many-electrode setups (Sec. IV). It complicates the phase dependence of the currents making it possible to distinguish different Andreev processes experimentally; (v) interplay of interaction-induced and common supercurrent in a two-constriction setup where the phase dependence manifests and distinguishes even more complex Andreev processes.

[1] K. v. Klitzing, G. Dorda, and M. Pepper, New Method for High-Accuracy Determination of the Fine-Structure Constant Based on Quantized Hall Resistance, Phys. Rev. Lett. **45**, 494 (1980).

[2] M. Z. Hasan and C. L. Kane, Colloquium, Rev. Mod. Phys. **82**, 3045 (2010).

[3] B. Huckestein, Scaling theory of the integer quantum Hall effect, Rev. Mod. Phys. **67**, 357 (1995).

[4] G. Murthy and R. Shankar, Hamiltonian theories of the fractional quantum Hall effect, Rev. Mod. Phys. **75**, 1101 (2003).

[5] T. H. Hansson, M. Hermanns, S. H. Simon, and S. F. Viefers, Quantum Hall physics: Hierarchies and conformal field theory techniques, Rev. Mod. Phys. **89**, 025005 (2017).

[6] J. Weis and K. von Klitzing, Metrology and microscopic picture of the integer quantum Hall effect, Philos. Trans. R. Soc., A **369**, 3954 (2011).

[7] Y. Takagaki, Transport properties of semiconductor-superconductor junctions in quantizing magnetic fields, Phys. Rev. B **57**, 4009 (1998).

[8] N. M. Chtchelkachev, Conductance of a semiconductor(2DEG) - superconductor junction in high magnetic field, JETP Lett. **73**, 94 (2001).

[9] M. Ma and A. Y. Zyuzin, Josephson effect in the quantum Hall regime, Europhys. Lett. **21**, 941 (1993).

[10] M. Stone and Y. Lin, Josephon currents in quantum Hall devices, Phys. Rev. B **83**, 224501 (2011).

[11] J. A. M. van Ostaay, A. R. Akhmerov, and C. W. J. Beenakker, Spin-triplet supercurrent carried by quantum Hall edge states through a Josephson junction, Phys. Rev. B **83**, 195441 (2011).

[12] F. Amet, C. T. Ke, I. V. Borzenets, J. Wang, K. Watanabe, T. Taniguchi, R. S. Deacon, M. Yamamoto, Y. Bomze, S. Tarucha, and G. Finkelstein, Supercurrent in the quantum Hall regime, Science **352**, 966 (2016).

[13] Y. Ji, Y. Chung, D. Sprinzak, M. Heiblum, D. Mahalu, and H. Shtrikman, An electronic Mach-Zehnder interferometer, Nature (London) **422**, 415 (2003).

[14] T. Jonckheere, P. Devillard, A. Crépieux, and T. Martin, Electronic Mach-Zehnder interferometer in the fractional quantum Hall effect, Phys. Rev. B **72**, 201305(R) (2005).

[15] G. Yang, Probing the $\nu = \frac{5}{2}$ quantum Hall state with electronic Mach-Zehnder interferometry, Phys. Rev. B **91**, 115109 (2015).

[16] F. Martins, S. Faniel, B. Rosenow, H. Sellier, S. Huant, M. G. Pala, L. Desplanque, X. Wallart, V. Bayot, and B. Hackens, Coherent tunneling across a quantum point contact in the quantum Hall regime, Sci. Rep. **3**, 1416 (2013).

[17] C.-Y. Hou, E.-A. Kim, and C. Chamon, Corner Junction as a Probe of Helical Edge States, Phys. Rev. Lett. **102**, 076602 (2009).

[18] C. W. J. Beenakker, Annihilation of Colliding Bogoliubov Quasiparticles Reveals their Majorana Nature, Phys. Rev. Lett. **112**, 070604 (2014).

[19] R. Riwar, M. Houzet, J. Meyer, and Y. V. Nazarov, Multiterminal Josephson junctions as topological matter, Nat. Commun. **7**, 1167 (2016).

[20] E. Eriksson, R.-P. Riwar, M. Houzet, J. S. Meyer, and Y. V. Nazarov, Topological transconductance quantization in a four-terminal Josephson junction, Phys. Rev. B **95**, 075417 (2017).

[21] T. Yokoyama and Y. V. Nazarov, Singularities in the Andreev spectrum of a multiterminal Josephson junction, Phys. Rev. B **92**, 155437 (2015).

[22] T. Yokoyama, J. Reutlinger, W. Belzig, and Y. V. Nazarov, Order, disorder, and tunable gaps in the spectrum of Andreev bound states in a multiterminal superconducting device, Phys. Rev. B **95**, 045411 (2017).

[23] E. Strambini, S. D'Ambrosio, F. Vischi, F. Bergeret, Y. V. Nazarov, and F. Giazotto, The omega-SQUIPT as a tool to phase-engineer Josephson topological materials, Nat. Nanotechnol. **11**, 1055 (2016).

[24] C. Padurariu, T. Jonckheere, J. Rech, R. Mélin, D. Feinberg, T. Martin, and Y. V. Nazarov, Closing the proximity gap in a metallic Josephson junction between three superconductors, Phys. Rev. B **92**, 205409 (2015).

[25] M. Amundsen, J. A. Ouassou, and J. Linder, Analytically determined topological phase diagram of the proximity-induced gap in diffusive n-terminal Josephson junctions, Sci. Rep. **7**, 40578 (2017).

[26] X.-L. Huang and Y. V. Nazarov, Supercurrents in Unidirectional Channels Originate from Information Transfer in the Opposite Direction: A Theoretical Prediction, Phys. Rev. Lett. **118**, 177001 (2017).

[27] Y. V. Nazarov and Y. M. Blanter, *Quantum Transport: Introduction to Nanoscience* (Cambridge University Press, Cambridge, UK, 2009).